IJMMM International Journal of Minerals, Metallurgy and Materials 矿物冶金与材料学报（英文版）

Electrochemistry of Hf(IV) in NaCl–KCl–NaF–K_2HfF_6 molten salts

Yan-ke Wu, Guo-qing Yan, Song Chen, and Li-jun Wang

Cite this article as:
Yan-ke Wu, Guo-qing Yan, Song Chen, and Li-jun Wang, Electrochemistry of Hf(IV) in NaCl–KCl–NaF–K_2HfF_6 molten salts, *Int. J. Miner. Metall. Mater.*, 27(2020), No. 12, pp. 1644-1649. https://doi.org/10.1007/s12613-020-2083-3

View the article online at SpringerLink or IJMMM Webpage.

Articles you may be interested in

Yun-long He, Rui-dong Xu, Shi-wei He, Han-sen Chen, Kuo Li, Yun Zhu, and Qing-feng Shen, Effect of $NaNO_3$ concentration on anodic electrochemical behavior on the Sb surface in NaOH solution, *Int. J. Miner. Metall. Mater.*, 25(2018), No. 3, pp. 288-299. https://doi.org/10.1007/s12613-018-1572-0

He Zhou, Yong-sheng Song, Wen-juan Li, and Kun Song, Electrochemical behavior of gold and its associated minerals in alkaline thiourea solutions, *Int. J. Miner. Metall. Mater.*, 25(2018), No. 7, pp. 737-743. https://doi.org/10.1007/s12613-018-1621-8

Wei Liu, Qing-he Zhao, and Shuan-zhu Li, Relationship between the specific surface area of rust and the electrochemical behavior of rusted steel in a wet-dry acid corrosion environment, *Int. J. Miner. Metall. Mater.*, 24(2017), No. 1, pp. 55-63. https://doi.org/10.1007/s12613-017-1378-5

Bao Liu, Shuo Wang, Cheng-yan Wang, Bao-zhong Ma, and Yong-qiang Chen, Electrochemical behavior and corrosion resistance of IrO_2–ZrO_2 binary oxide coatings for promoting oxygen evolution in sulfuric acid solution, *Int. J. Miner. Metall. Mater.*, 27(2020), No. 2, pp. 264-273. https://doi.org/10.1007/s12613-019-1847-0

Chun-fa Liao, Yun-fen Jiao, Xu Wang, Bo-qing Cai, Qiang-chao Sun, and Hao Tang, Electrical conductivity optimization of the Na_3AlF_6-Al_2O_3-Sm_2O_3 molten salts system for Al-Sm intermediate binary alloy production, *Int. J. Miner. Metall. Mater.*, 24(2017), No. 9, pp. 1034-1042. https://doi.org/10.1007/s12613-017-1493-3

IJMMM WeChat

QQ author group

International Journal of Minerals, Metallurgy and Materials
Volume 27, Number 12, December 2020, Page 1644
https://doi.org/10.1007/s12613-020-2083-3

Electrochemistry of Hf(IV) in NaCl–KCl–NaF–K_2HfF_6 molten salts

Yan-ke Wu, Guo-qing Yan, Song Chen, and Li-jun Wang

GRINM Resources and Environment Tech. Co., Ltd, Beijing 101407, China
(Received: 19 March 2020; revised: 21 April 2020; accepted: 26 April 2020)

Abstract: The cathodic reduction mechanism of Hf(IV) ions in a fused NaCl–KCl–NaF–K_2HfF_6 salt system was studied in various NaF concentrations at 1073 K to obtain a purified dendritic Hf metal. The results of cyclic voltammetry and square wave voltammetry indicated that the reduction process comprised two steps of Hf(IV) → Hf(II) and Hf(II) → Hf at low NaF concentrations (0 < molar ratio of $[F^-/Hf^{4+}] \leq 17.39$) and one step of Hf(IV) → Hf at high NaF concentrations (17.39 < molar ratio of $[F^-/Hf^{4+}] < 23.27$). The structure and morphology of the deposits obtained in potentiostatic electrolysis in the one-step reduction process were analyzed and verified by X-ray diffraction, scanning electron microscopy, and energy dispersive X-ray spectrometry. In the one-step reduction process, the disproportionation reaction between the Hf metal and Hf complex ions was inhibited, and a large dendrite Hf metal was achieved in molten salt electrorefining.

Keywords: electrochemical behavior; cyclic voltammetry; potentiostatic electrolysis; dendritic hafnium; molten salts

1. Introduction

Hafnium (Hf) has a considerably large neutron absorption cross section (1.05×10^{-26} m^2) that is nearly 600 times that of zirconium (Zr); it is mainly used in control and emergency shutdown rods in nuclear reactors [1–2]. High-purity Hf has also been used as a target in preparing HfO_2 films. HfO_2 films are characterized by a high refractive index, high absorption, and low laser-induced damage threshold; moreover, they have been used to prepare high-power laser films [3]. HfO_2 and Hf-based oxides have been recently highlighted as the most suitable dielectric materials because of their comprehensive performance [4–5]. Molten salt electrorefining is one of the most important methods to prepare high-purity Hf metal and effectively remove impurities, such as Fe, Cr, and Mn.

The electrochemistry of Hf(IV) in NaCl–KCl–K_2HfF_6 and NaCl–KCl–NaF–K_2HfF_6 molten salt has been widely investigated. Chen *et al.* [6] suggested the electrochemical reduction of Hf(IV) complex ions in chloride and chloride–fluoride melts with low fluoride content (0 < molar ratio of $[F^-/Hf^{4+}] < 6$) via two steps of Hf(IV) → Hf(II) and Hf(II) → Hf; for high fluoride concentrations (molar ratio of $[F^-/Hf^{4+}] > 16$), another step of Hf(IV) → Hf is necessary. Poinso *et al.* [7] discovered that hafnium tetrachloride ($HfCl_4$) dissolved in an equimolar mixture of NaCl–KCl molten salt can be reduced to metallic Hf via a one-step process at the temperature range of 973–1173 K. In our previous works [8–9], the molten salt electrochemical reduction of Hf(IV) complex ions in NaCl–KCl–K_2HfCl_6 was investigated. The results revealed that the reduction process involves two steps, namely, Hf(IV) → Hf(II) and Hf(II) → Hf.

As $HfCl_4$ has a low volatilization point (592 K), K_2HfF_6 was chosen in the current work as a raw material for refining Hf metal. The Hf electrorefining experiment on NaCl–KCl–K_2HfF_6 molten salt was conducted in our previous works, but only Hf powder was obtained in the cathode deposit. On the basis of the research results in the literature [6], we propose a method for realizing a one-step reduction of Hf(IV) complex ions through the addition of specific proportions of NaF to the NaCl–KCl–K_2HfF_6 system so as to obtain large-scale dendritic Hf metals. The purpose of our investigation is to determine the electrochemical behavior of Hf(IV) complex ions in NaCl–KCl–NaF–K_2HfF_6 molten salt at different NaF concentrations and ascertain the optimum $[F^-/Hf^{4+}]$ proportion.

2. Experimental

2.1. Preparation and purification of molten salt

The molten salt consisted of a eutectic NaCl–KCl mixture (Alfa Aesar, 99.9% purity, molar ratio: 1:1). The salts were pre-dried under a vacuum for 24 h at 773 K to remove the water content. Before each experiment, HCl was bubbled in-

Corresponding author: Yan-ke Wu E-mail: luckwyk@163.com

to the fused salt to further eliminate the dissolved water. Hf ions were added into the bath in the form of potassium fluorohafnate (K_2HfF_6, 99.9% purity) pellets, and NaF was added into the bath to change the fluoride ion concentration.

2.2. Electrochemical apparatus and electrodes

All electrochemical measurements were performed using the Zahner IM6 electrochemical workstation with the software package Thales XT 5.2.0. The reference electrode was prepared by inserting a silver wire (ϕ1 mm, Alfa Aesar, 99.99% purity) into a 8 mm-diameter mullite tube filled with NaCl–KCl eutectic salts containing AgCl (1wt%). A polished platinum (Pt) wire (ϕ1 mm, Alfa Aesar, 99.99% purity) serving as a working electrode was cleaned ultrasonically with deionized water and alcohol and then subsequently dried before use. The surface area of the working electrode was determined by controlling the depth of the electrode immersion. A pyrolytic graphite crucible was used as the counter electrode.

All experiments were conducted in a protective purified argon atmosphere. The cathodic reduction mechanism of Hf(IV) complex ions at different NaF concentrations in the NaCl–KCl–NaF–K_2HfF_6 system was studied using a Pt wire working electrode, Ag/AgCl reference electrode, and pyrolytic graphite auxiliary electrode at 1023 K.

The apparatus is shown in Fig. 1. The temperature of the salts was monitored with a nickel–chromium thermocouple, and the temperature fluctuation was maintained at ±1 K. The deposits by potentiostatic electrolysis on the Pt electrode were identified by X-ray diffraction (XRD). The morphology of the Hf deposits was characterized by scanning electron microscopy (SEM), and microzone chemical analysis was performed using energy dispersive X-ray spectrometry (EDS).

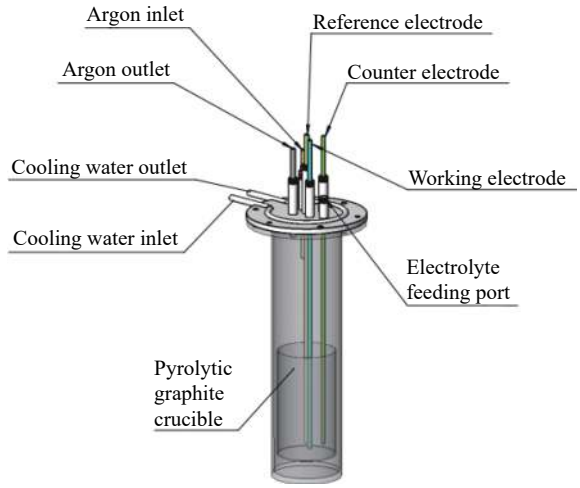

Fig. 1. Schematic view of experimental apparatus.

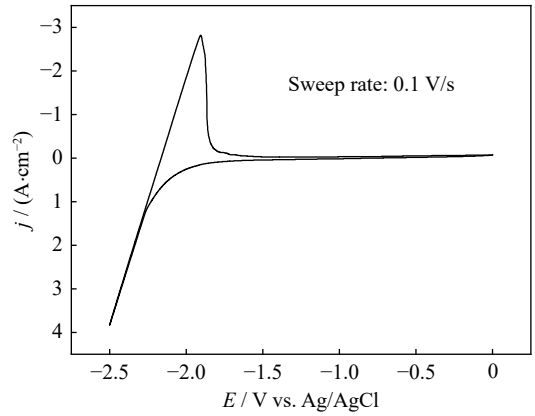

Fig. 2. Cyclic voltammogram in eutectic NaCl–KCl molten salt at 1073 K. Working electrode (0.1650 cm^2): Pt wire.

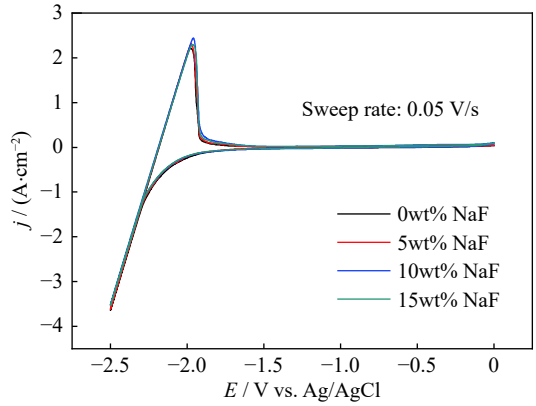

Fig. 3. Cyclic voltammogram of NaCl–KCl–NaF molten salt with different NaF concentrations at 1073 K. Working electrode (0.1650 cm^2): Pt wire.

3. Results and disussion

3.1. Electrochemical behavior of Hf(IV) ions in NaCl–KCl–NaF–K_2HfF_6

3.1.1. Cyclic voltammetry analysis

The cyclic voltammetry curves of eutectic NaCl–KCl molten salt were studied. As shown in Fig. 2, when the potential shifted to −1.9 V vs. Ag/AgCl, the current density began to increase. This result indicated that alkali metal ions were reduced. Therefore, the cathode reduction potential of Hf(IV) in NaCl–KCl–K_2HfF_6 should be controlled in the potential range of 0 to −1.9 V vs. Ag/AgCl. In Fig. 2, j is the current density and E is the electrode potential.

The blank potential window in NaCl–KCl–NaF molten salt with different fluoride concentrations was also studied. The results are shown in Fig. 3.

The potential window of the NaCl–KCl–NaF molten salt system basically remained the same. Hence, the reduction potential of Hf(IV) complex ions was not disturbed in the potential range of 0 to −1.9 V when the NaF concentration was less than 15wt%.

The cyclic voltammograms of NaCl–KCl–NaF–K_2HfF_6 molten salt with different NaF concentrations of 5wt%,

10wt%, and 15wt% are shown in Fig. 4. The reduction potentials of Hf(IV) complex ions obtained from Fig. 4 are shown in Fig. 5. The deposition potential of Hf(IV) complex ions gradually shifted negatively with the increase of NaF concentration.

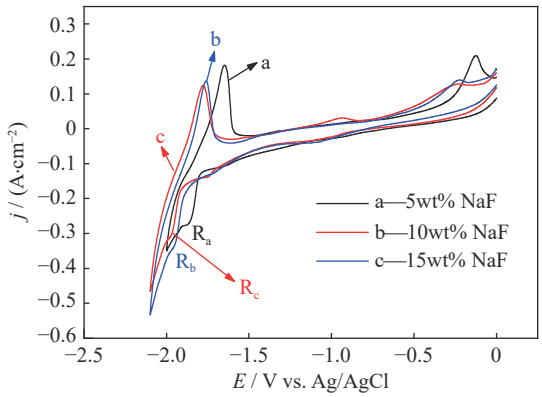

Fig. 4. Cyclic voltammogram of K_2HfF_6 (1.559×10^{-4} mol·cm^{-3}) in NaCl–KCl–NaF–K_2HfF_6 molten salt with different NaF concentrations at 1073 K. R_a, R_b, and R_c means the reduction peak in the curve a, b, and c, respectively. Working electrode (0.1650 cm^2): Pt wire.

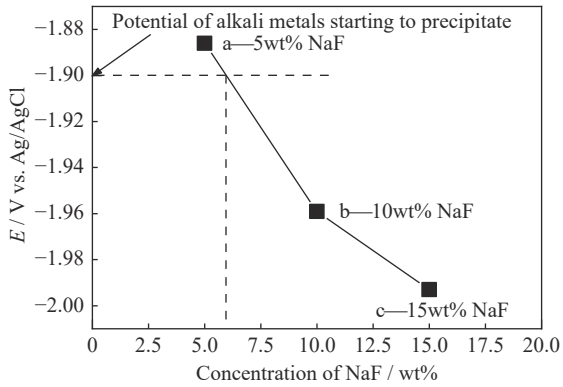

Fig. 5. Dependence of deposition potential of Hf (IV) complex ions on NaF concentration.

When NaF concentration exceeded 5.94wt% (molar ratio of [F^-/Hf^{4+}] = 23.27), the alkali metals began to reduce. Therefore, the concentration of NaF should be less than 5.94wt% during the electrorefinement of Hf in NaCl–KCl–NaF–K_2HfF_6 molten salt. Therefore, cyclic voltammetry was conducted in molten salt with 3wt% and 4wt% NaF to determine the minimum concentration of NaF for the one-step reduction of Hf(IV) complex ions in NaCl–KCl–NaF–K_2HfF_6 molten salt (Fig. 6).

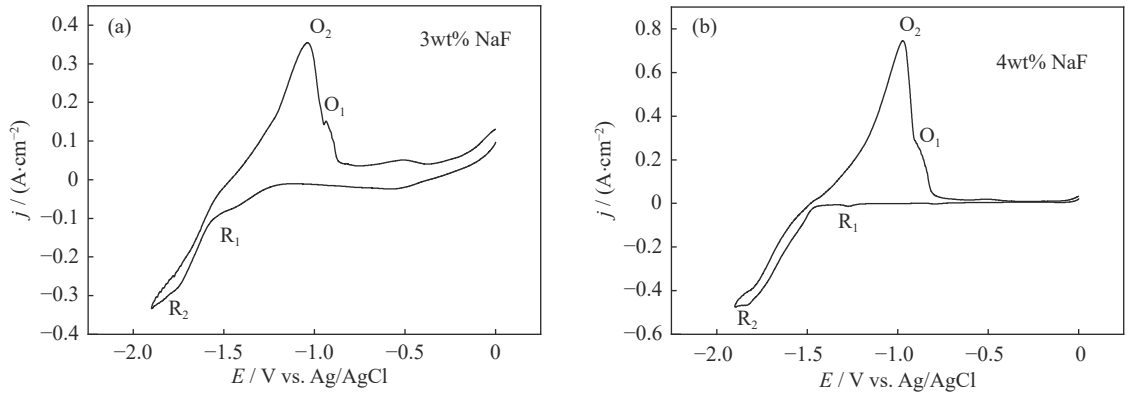

Fig. 6. Cyclic voltammogram of K_2HfF_6 (1.559×10^{-4} mol·cm^{-3}) in NaCl–KCl–NaF–K_2HfF_6 molten salt with different NaF concentrations at 1073 K: (a) 3wt% NaF; (b) 4wt% NaF. R_1 and R_2 represent the reduction peaks, and O_1 and O_2 represent the oxidation peaks of Hf(IV) complex ions. Sweep rate: 0.05 V/s; working electrode (0.1650 cm^2): Pt wire.

Fig.6 shows that when the NaF concentration was 3wt% ([F^-/Hf^{4+}] = 14.72), two reduction peaks (R_1 and R_2) were observed. However, when the NaF concentration was 4wt% ([F^-/Hf^{4+}] = 17.39), the current of peak R_1 was close to zero, which is close to a one-step reduction process. The cyclic voltammetric curves of Hf(IV) complex ions at different scanning rates with NaF concentration of 5wt% ([F^-/Hf^{4+}] = 20.39) are plotted in Fig.7, and the data of the reduction peak R obtained from Fig. 7 are listed in Table 1. The reduction peak potential ($E_{p,R}$) moved slightly to the negative direction with the increase of scanning rate.

The relationship between the current density of peak R and the square root of sweep rate ($v^{1/2}$) is shown in Fig. 8. It shows that the peak current density was proportional to the square root of the sweep rate. Hence, the reduction of Hf^{4+} complex ions was found to be under diffusion control [10–12].

In a diffusion-controlled reversible process, the electron transfer number can be calculated by the following equation [13–14]:

$$E_{p/2} = E_p + 2.2(RT/nF) \quad (1)$$

where $E_{p/2}$ is the half peak potential, E_p is the peak potential, R is the real gas constant (8.314 J·mol^{-1}·K^{-1}), T is the temperature (K), n is the number of electrons involved in the reaction, and F is the Faraday constant.

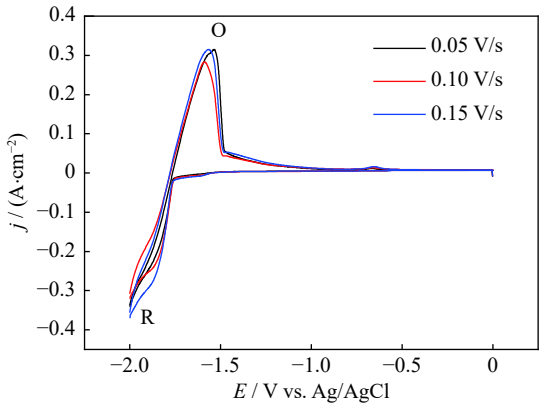

Fig. 7. Cyclic voltammogram of K_2HfF_6 (1.559 × 10^{-4} mol·cm^{-3}) in NaCl–KCl–5wt%NaF–K_2HfF_6 molten salt at 1073 K at different scanning rates. Working electrode (0.1590 cm^2): Pt wire.

Table 1. Cyclic voltammetric curve data of peak R at various scanning rates

Scanning rate / ($V·s^{-1}$)	j_p / ($A·cm^{-2}$)	$E_{p,R}$ / V	$E_{p/2,R}$ / V	ΔE / V
0.05	0.2165	−1.873	−1.826	0.047
0.10	0.2406	−1.875	−1.826	0.049
0.15	0.2534	−1.877	−1.827	0.050

Note: j_p is the peak current density; $E_{p/2,R}$ is the half reduction peak potential; ΔE *is* the difference between the value of $E_{p/2,R}$ and $E_{p,R}$.

The electron transfer number of peak R was calculated according to Eq. (1), and the results are shown in Table 2. It indicates that the number of electrons relative to peak R of Hf^{4+} complex ions in the NaCl–KCl–K_2HfF_6–5wt%NaF molten salt system is 4. Hence, the cathodic reduction process is $Hf^{4+} + 4e \rightarrow Hf$.

Table 2. Electron transfer number of peak R at various scanning rates

Scanning rate / ($V·s^{-1}$)	$E_{p,R}$ / V	$E_{p/2,R}$ / V	$2.2RT/F$	ΔE / V	n
0.05	−1.873	−1.826	0.1939	0.047	4.13
0.10	−1.875	−1.826	0.1939	0.049	3.96
0.15	−1.877	−1.827	0.1939	0.050	3.88

The results shown in the above indicates that Hf(IV) complex ions were reduced to metallic Hf via two steps of Hf(IV) → Hf(II) and Hf(II) → Hf at low NaF concentrations ($0 < [F^-/Hf^{4+}] \leq 17.39$). At high NaF concentrations ($17.39 < [F^-/Hf^{4+}] < 23.27$), a one-step reduction mechanism corresponding to Hf(IV) → Hf was achieved.

3.1.2. Square wave voltammetry analysis

Square wave voltammetry was conducted at 1073 K to further verify the reduction mechanism. The results are shown in Fig. 9. As shown in Fig. 9, one reduction peak was observed; it is consistent with the result of the cyclic voltammogram in Fig. 7. The number of electrons involved in the electrochemical step was determined by square wave voltammetry. For a simple reversible reaction, the electron transfer number can be calculated according to the following equation [15–16]:

$$W_{1/2} = 3.52RT/nF \quad (2)$$

where $W_{1/2}$ is the half peak width.

As shown in Table 3, the electron transfer number corresponding to peak R is approximately 4, which is also consistent with that obtained by cyclic voltammetry.

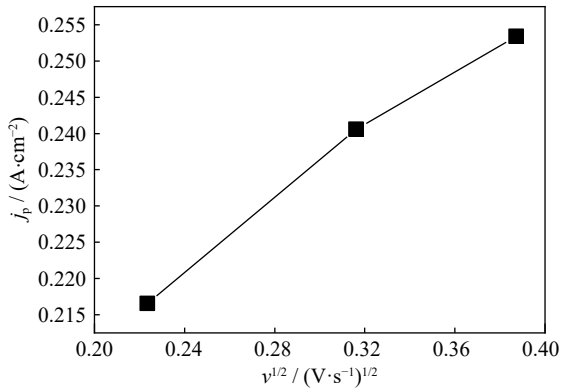

Fig. 8. Dependence of peak current density (j_p) on square root of sweep rate.

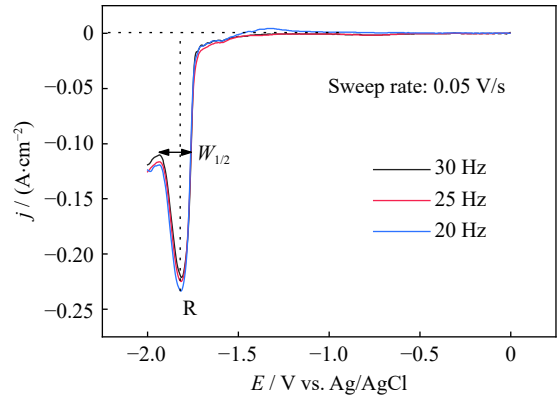

Fig. 9. Square wave voltammetric curves of K_2HfF_6 (1.559 × 10^{-4} mol·cm^{-3}) at different frequencies in NaCl–KCl–5wt%NaF–K_2HfF_6. Working electrode (0.1590 cm^2): Pt; pulse height: 25 mV; potential step: 1 mV.

3.2. Potentiostatic electrolysis verification

Potentiostatic electrolysis was carried out at −1.88 V vs.

Table 3. Electron transfer number calculated from different square wave voltammetric frequencies

Frequency / Hz	$3.52RT/F$	E_p / V	$W_{1/2}$ / V	n
20	0.3103	−1.812	0.078	3.978
25	0.3103	−1.816	0.080	3.879
30	0.3103	−1.816	0.076	4.083

Ag/AgCl, which is slightly more negative than the deposition potential of Hf(IV) ions. After electrolysis, the products were cleaned to remove the bonded electrolyte and then analyzed. From the XRD pattern in Fig. 10, Hf, Pt, HfPt, and Hf_2Pt were detected; this result is in agreement with the phase diagram of Pt–Hf binary alloys [17].

Products with large grain sizes were obtained (Fig.11). It means that when the concentration of fluoride ($17.39 < [F^-/Hf^{4+}] < 23.27$) reached a certain value, the Hf(IV) complex ions were reduced to metallic Hf via a one-step process.

Theoretically, Hf(IV) complex ions exist in the NaCl–KCl–K_2HfF_6 melt in the form of $[HfCl_mF_n^{2-}]$ ($m + n = 6$). When the concentration of NaF increases, $[F^-]$ gradually replaces the position of $[Cl^-]$, and $[HfCl_mF_n^{2-}]$ changes to $[HfF_6^{2-}]$due to the high thermodynamic stability of $[HfF_6^{2-}]$. Therefore, when the concentration of NaF is high, Hf(IV) complex ions mainly exist in the form of $[HfF_6^{2-}]$, and the disproportionation reaction between Hf and Hf(IV) complex ions is reduced.

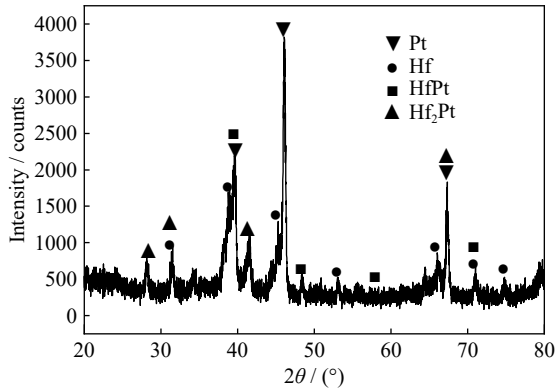

Fig. 10. XRD pattern of products on Pt electrode after 3 h of potentiostatic electrolysis at −1.88 V vs. Ag/AgCl.

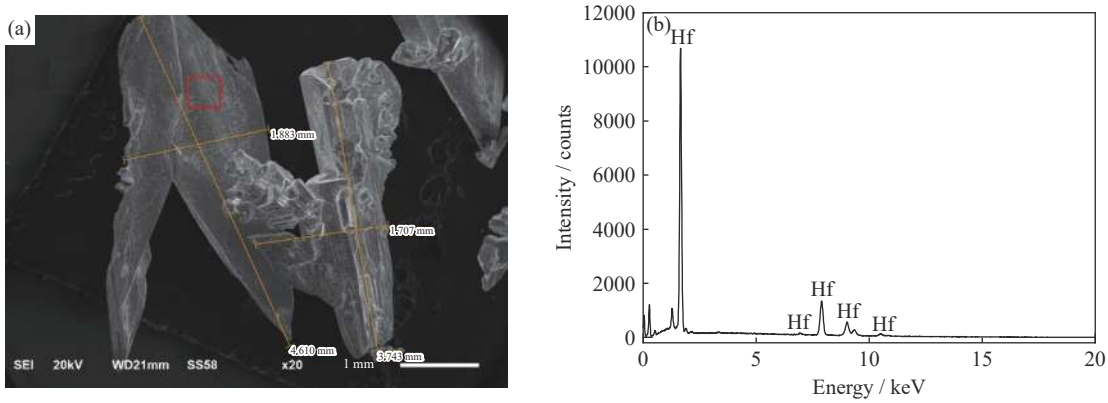

Fig. 11. SEM and EDS analyses of deposited Hf metal by potentiostatic electrolysis at −1.88 V vs. Ag/AgCl.

4. Conclusions

The electrochemistry of Hf(IV) complex ions in NaCl–KCl–NaF–K_2HfF_6 molten salt was studied at 1073 K according to cyclic voltammetry analysis and square wave voltammetry analysis. The main findings are presented as follows.

(1) Hf(IV) complex ions were reduced to metallic Hf via two steps of Hf(IV) → Hf(II) and Hf(II) → Hf at low NaF concentrations ($0 < [F^-/Hf^{4+}] \leq 17.39$). At high NaF concentrations ($17.39 < [F^-/Hf^{4+}] < 23.27$), a one-step reduction mechanism corresponding to Hf(IV) → Hf was achieved.

(2) The deposits products after electrodeposition at −1.88 V vs. Ag/AgCl are the Hf and Pt–Hf compounds, which coincided with the phase diagram of the binary alloy of Pt and Hf.

(3) At high NaF concentrations, potentiostatic electrolysis was conducted with a one-step reduction process because the disproportionation reaction between Hf(IV) complex ions and the Hf metal was reduced, and relatively large-scale dendritic products were obtained.

Acknowledgement

This work was financially supported by the National Natural Science Foundation of China (No. 51204021).

References

[1] T. Iwasakl and K. Konashi, Development of hydride absorber for fast reactor-application of hafnium hydride to control rod of large fast reactor, *J. Nucl. Sci. Technol.*, 46(2009), No. 8, p. 874.

[2] T. R. Tricot, The metallurgy and functional properties of hafnium, *J. Nucl. Mater.*, 189(1992), No. 3, p. 277.

[3] M. Zukic, D.G. Torr, J.F. Spann, and M.R. Torr, Vacuum ultraviolet thin films. Ⅰ—Optical constants of BaF_2, CaF_2, LaF_3, MgF_2, Al_2O_3, HfO_2, and SiO_2 thin films, *Appl. Opt.*, 29(1990), No. 28, p. 4284.

[4] A. Srivastava, R.K. Nahar, and C.K. Sarkar, Study of the effect of thermal annealing on high k hafnium oxide thin film structure and electrical properties of MOS and MIM devices, *J. Mater. Sci.-Mater. Electron.*, 22(2011), No. 7, p. 882.

[5] J.H. Choi, Y. Mao, and J.P. Chang, Development of hafnium based high-*k* materials—A review, *Mater. Sci. Eng. R*, 72

(2011), No. 6, p. 97.

[6] G.S. Chen, O. Masazumi, and O. Takeo, Electrochemical studies of zirconium of zirconium and hafnium in alkali chloride and alkali fluoride-chloride molten salts, *J. Appl. Electrochem.*, 20(1990), No. 1, p. 77.

[7] J.Y. Poinso, S. Bouvet, P. Ozil, J.C. Poignet, and J. Bouteillon, Electrochemical reduction of hafnium tetrachloride in molten NaCl–KCl, *J. Electrochem. Soc.*, 140(1993), No. 5, p. 1315.

[8] X. Liu, Y.K. Wu, S. Chen, B. Song, and L.J. Wang, Electrochemical reduction behavior of Hf(IV) in molten NaCl–KCl–K_2HfCl_6 system, *Rare Met.*, 35(2016), No. 8, p. 655.

[9] Y.K. Wu, Z.G. Xu, S. Chen, L.J. Wang, and G.X. Li, Electrochemical behavior of zirconium in molten NaCl–KCl–K_2ZrF_6 system, *Rare Met.*, 30(2011), No. 1, p. 8.

[10] A. Novoselova and V. Smolenski, Electrochemical behavior of neodymium compounds in molten chlorides, *Electrochim. Acta.*, 87(2013), p. 657.

[11] R.B. Prabhakara, S. Vandarkuzhali, T. Subramanian, and P. Venkatesh, Electrochemical studies on the redox mechanism of uranium chloride in molten LiCl–KCl eutectic, *Electrochim Acta.*, 49(2004), No. 15, p. 2471.

[12] L. Cassayre, J. Serp, P. Soucek, R. Malmbeck, J. Rebizant, and J.P. Glatz, Electrochemistry of thorium in LiCl–KCl eutectic melts, *Electrochim*, *Acta*, 52(2007), No. 26, p. 7432.

[13] L.P. Polyakova, P. Taxil, and E.G. Polyakov, Electrochemical behavior and codeposition of titanium and niobium in chloride-fluoride melts, *J. Alloys Compd.*, 359(2003), No. 1-2, p. 244.

[14] R.S. Nicholson and I. Shain, Theory of stationary electrode polarography: single scan and cyclic methods applied to reversible, irreversible, and kinetic systems, *Anal. Chem.*, 36(1964), No. 4, p. 706.

[15] A.J. Bard and L.R. Faulkner, *Electrochemical Methods: Fundamentals and Applications*, 2nd ed., John Wiley & Sons, Inc., New York, 2001.

[16] C. Hamel, P. Chamelot, and P. Taxil, Neodymium(Ⅲ) cathodic process in molten fluoride, *Electrochim. Acta*, 49(2004), No. 25, p. 4467.

[17] J.K. Stalick and R.M. Waterstrat, The hafnium-platinum phase diagram, *J. Phase Equilib. Diffus.*, 35(2014), No. 1, p. 15.